PICTURES OF THE MICROWAVE BACKGROUND FLUCTUATIONS

G. Efstathiou

Institute of Astronomy
Madingley Road
Cambridge CB3 OHA
England

1. Introduction

Modern theories of particle physics have now progressed sufficiently that it is possible to compute the nature of small irregularities that may explain the origin of galaxies. Although these calculations are hardly definitive, they have succeeded in drawing attention to a particular set of initial conditions, namely adiabatic scale-invariant Gaussian fluctuations superimposed on an $\Omega = 1$ Friedman background (see e.g. Guth and Pi, 1982; Hawking, 1982; Bardeen, Steinhardt and Turner, 1983).

Such fluctuations should generate a highly specific pattern in the microwave background radiation. The statistical properties of the microwave background anisotropies (e.g. the temperature autocorrelation function, number density of hot spots) could therefore provide a clear and definitive test of theories of the early universe.

The failure to observe fluctuations in the background radiation has already led to interesting constraints on theories of galaxy formation. Present upper limits on temperature anisotropies on small angular scales ($\Delta T/T \lesssim 3\times10^{-5}$, $\Delta\vartheta = 4.5'$, Uson and Wilkinson 1984a,b) essentially exclude models in which the density of the universe is dominated by ordinary baryonic matter (Wilson and Silk, 1981), provided that reionization of the inter-galactic medium at redshifts $z \gtrsim 30$ has not been effective at erasing the background fluctuations. Even if we assume that exotic weakly interacting dark matter, such as gravitinos, photinos, axions etc., dominate over the baryonic component, our failure to observe small-scale anisotropies implies a relatively high density universe with $\Omega \gtrsim 0.2$ (Bond and Efstathiou, 1984; Vittorio and Silk, 1984; Efstathiou and Bond, 1986a). More powerful constraints could be obtained from sensitive experiments on scales $\vartheta >$

1°, since anisotropies on these angular scales would be unaffected by secondary reionization and are closely related to the shape of the initial fluctuation spectrum.

In this article we will attempt to give the reader a feel for the characterstic features of the background radiation pattern expected from scale-invariant perturbations by generating numerical realizations of the radiation intensity. These allow us to translate the relatively complex calculations of the radiation fluctuations into a form that is more easily digestible by non-experts. It will become apparent that many of the background anisotropy experiments have not been designed to maximise the signal expected from scale-invariant fluctuations, and it will be easy to see how (in theory!) better experiments could be constructed. In addition, it is relatively straightforward to visualize how the radiation pattern would be altered by departures from a scale-invariant spectrum. A technical account of the statistics of the microwave background fluctuations is given by Bond and Efstathiou (1986).

2. The Autocorrelation Function of the Temperature Fluctuations

It is natural to express the temperature pattern on the celestial sphere using spherical harmonics,

$$\Delta T(\vartheta,\varphi)/T = \sum a_\ell{}^m Y_\ell{}^m(\vartheta,\varphi) \quad . \tag{1}$$

Now consider the temperature autocorrelation function

$$C_T(\vartheta) = \langle \Delta T/T(\hat{\gamma}_1)\Delta T/T(\hat{\gamma}_2)\rangle \ , \quad \hat{\gamma}_1\cdot\hat{\gamma}_2 = \cos\vartheta \ , \tag{2}$$

where the brackets denote an ensemble average. We expect the coefficients $a_\ell{}^m$ in (1) to be statistically independent. Thus we define a spectral coefficient

$$c_T(\ell) = \frac{1}{(2\ell+1)}\sum_m |a_\ell{}^m|^2 \ , \tag{3}$$

which is related to the autocorrelation function according to

$$C_T(\vartheta) = \frac{1}{4\pi}\sum_\ell (2\ell+1)c_T(\ell)\, P_\ell(\cos\vartheta) \quad . \tag{4}$$

Since the photons are coupled to the matter by Thomson scattering, we expect the fluctuating part of the radiation field to be linearly polarized (Kaiser, 1983). This may be characterized by the Stokes parameter Q (in a suitably chosen coordinate system) fixing the degree of polarization at each point on the sky.

We may then define an analogous autocorrelation function $C_P(\vartheta)$ with power-spectrum $c_P(\ell)$ to describe the statistical properties of the fractional polarization.

If we now assume that the initial fluctuations are Gaussian, then the spherical harmonic coefficients a_ℓ^m will be Gaussian distributed with zero mean. Thus, if we can determine either the autocorrelation functions $C(\vartheta)$ or the power-spectra $c(\ell)$, we will be able to specify statistically almost all aspects of the radiation pattern.

The computation of $C(\vartheta)$ proceeds as follows (see Bond and Efstathiou, 1986, for a detailed account). We specify the perturbation to the photon distribution function $\delta f_\gamma = (T\partial\bar{f}/\partial T)\,\Delta_T/4$, together with a similar expression for the polarization amplitude. Here, $\bar{f}$ is the unperturbed photon distribution function. If the background metric is assumed to be flat, we can decompose the initial perturbations into a sum of plane waves. The Boltzmann equation for the radiation, including gravitational terms and Thomson scattering, is then solved numerically. The evolution of Δ_T depends on the direction of propagation of the photons relative to the wave vector **k**. Therefore, we expand Δ_T in terms of Legendre polynomials

$$\Delta_T(k,\mu) = \sum_\ell (2\ell+1)\alpha_\ell\,(k,\tau)\,P_\ell(\mu)\ , \qquad \mu = \cos\vartheta\ , \tag{5}$$

keeping only as many terms as are necessary for accurate solutions ($\ell_{max} \sim k\tau$). In (5) τ is conformal time $\tau = \int dt/a$, where a is the scale-factor of the background metric. The autocorrelation function is given by

$$C_T(\vartheta) = \frac{V_x}{32\pi^2}\int_0^\infty \sum_\ell (2\ell+1)\left|\alpha_\ell(k,\tau_o)\right|^2\ P_\ell\,(\cos\vartheta)k^2dk \tag{6}$$

and the power-spectrum is given by

$$c_T(\ell) = \frac{V_x}{8\pi}\int_0^\infty \left|\alpha_\ell(k,\tau_o)\right|^2\,k^2dk \tag{7}$$

where τ_o denotes the present time and we assume that the perturbations are periodic in a large box of volume V_x.

At large angular scales (greater than the width of the last scattering surface $\vartheta > 1°$) , the dominant contribution to the radiation anisotropy arises from the Sachs-Wolfe effect (Sachs and Wolfe, 1967; Peebles, 1982). This gives

$$\Delta_T \approx -\frac{2\dot{h}}{k^2} e^{-ik\mu\tau} \quad , \tag{8}$$

where h is the trace of the metric perturbation and dots denote derivatives with respect to τ. If the initial fluctuation spectrum is scale-invariant ($<|h(\tau_i)|^2> \propto k$), the autocorrelation function at large angular scales will be given by

$$C_T(\vartheta) \approx \frac{3a_2^2}{2\pi} \left\{ \ell n \left(\frac{2}{1-\cos\vartheta}\right) - 1 - 3/2 \cos\vartheta \right\} \quad , \tag{9}$$

where a_2 is the amplitude of the quadrupole component (equation (1)) and we have subtracted the contribution from the monopole and dipole terms. (The monopole term is, of course, unobservable; the dipole term in the observed radiation pattern is dependent on our motion relative to the comoving frame which we know is influenced by the distribution of nearby matter).

If the initial spectrum is not scale invariant, $<|h|^2> \propto k^n$, the radiation power spectrum is

$$c_T(\ell) = a_2^2 \frac{\Gamma\left(\frac{9-n}{2}\right)}{\Gamma\left(\frac{n+3}{2}\right)} \frac{\Gamma\left(\ell+\left(\frac{n-1}{2}\right)\right)}{\Gamma\left(\ell+\left(\frac{5-n}{2}\right)\right)} \quad , \tag{10}$$

for $n < 3$. (If $n \geq 3$, the power-spectrum at all ℓ is dependent on the exact behaviour of the radiation field at large wavenumbers). Evidently if $\ell \gg 1$, $c_T(\ell) \propto \ell^{(n-3)}$. Thus, the large-angle properties of the radiation field should be a sensitive indicator of the form of the initial fluctuation spectrum.

On smaller angular scales, Thomson scattering is important and we must resort to a numerical solution of the Boltzmann equation to determine $C(\vartheta)$. In Figure (1) we show autocorrelation functions in an $\Omega = 1$ model with scale-invariant adiabatic fluctuations in which the present density is dominated by cold dark matter ($\Omega = 1$); the Hubble constant is $h = 0.75$ ($h = H_o/75$ km s^{-1} Mpc^{-1}), and baryons contribute $\Omega_B = 0.03$. The corresponding power-spectra are shown in Figure (2). Notice the high degree of coherence in $C_T(\vartheta)$; the amplitude falls by only an order of magnitude between 0 and $\sim 9°$. This is a key feature of the radiation pattern arising from scale-invariant fluctuations. At larger angles, the correlation function follows the double-humped behaviour of equation (9). In contrast, the polarization is correlated only on small scales ($\lesssim 10'$).

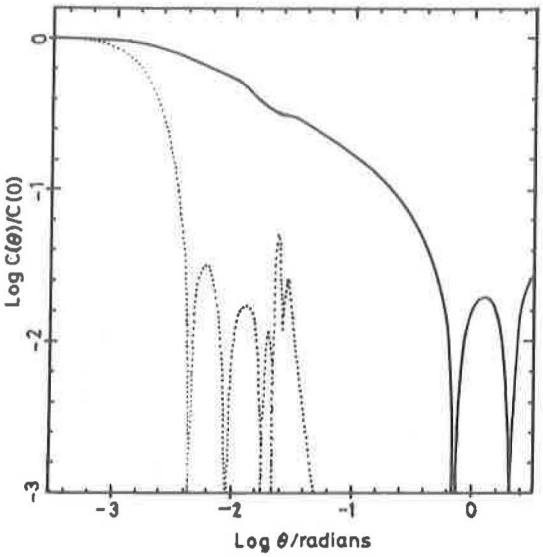

Figure 1. Autocorrelation function for the temperature fluctuations (solid line) and for the polarization fluctuations (dashed line) in an $\Omega = 1$ cold dark matter model with scale-invariant adiabatic fluctuations.

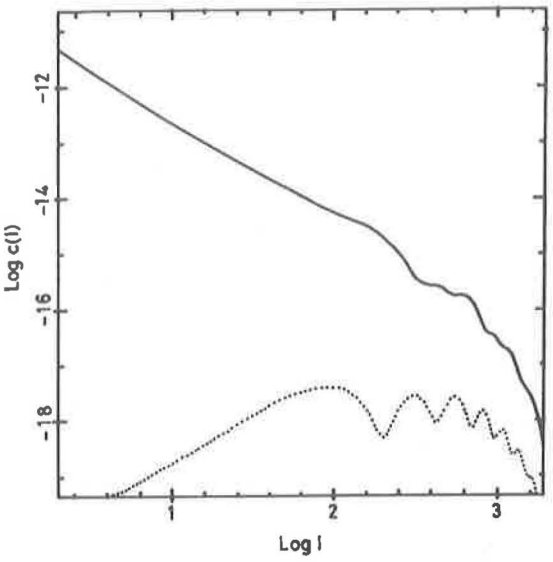

Figure 2. Power-spectra corresponding to the autocorrelation functions shown in Figure 1.

3. Numerical Simulations

Having derived the power-spectra, we can now make simulated maps of the sky via equation (1). However, for large ℓ, this is impractical since evaluating high-order spherical harmonics is extremely demanding computationally. Instead, we consider the small-angle limit of equation (4)

$$\hat{C}_T(\vartheta) \approx \frac{1}{4\pi} \sum_{\ell} (2\ell+1)\, c_T(\ell)\, J_0(\ell\vartheta) \qquad (11)$$

If the dominant contribution to $\hat{C}_T$ comes from $\ell >> 1$, or if the sum is restricted to high ℓ, then equ. (11) corresponds to a two-dimensional Fourier transform. A Euclidean map with expected correlation function $\hat{C}_T$ can thus be generated by selecting the amplitudes of $c(\ell)^{\frac{1}{2}}$ from a Gaussian distribution and assigning phases at random in the interval $(0,2\pi)$. Simulations of the power-spectra are shown in Figure (3). The resulting maps of a square patch of sky of side 10° are shown in Figures (4) and (5). These maps show clearly the features described above, namely the high degree of spatial correlation of the total radiation intensity and the small-scale coherence of the polarization.

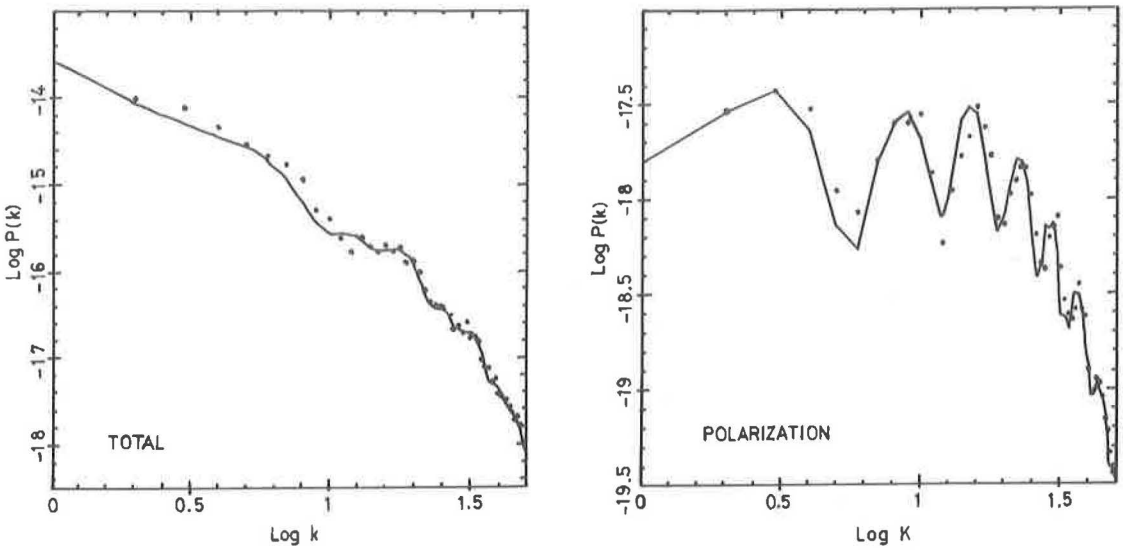

Figure 3. The filled circles show the power-spectra of a numerical simulation with Gaussian statistics designed to match the theoretical spectra (solid lines). (a) shows the total radiation fluctuation spectrum and (b) shows the polarization spectrum.

Even though these maps represent a cold dark matter dominated Universe with Ω = 1, the r.m.s. fluctuation in the background radiation should be within detectable limits if galaxies and clusters formed by gravitational instability. The amplitude of the initial fluctuation spectrum may be fixed by comparing with the second moment of the galaxy correlation function $J_3 = \int \xi\, x^2 dx$ integrated out to some suitably large scale ($x_o \sim 10h^{-1}$Mpc, see Bond and Efstathiou, 1984). We will use this procedure in the numerical estimates quoted below. However, this may lead us to overestimate the temperature anisotropy, perhaps by as much as a factor of two, if galaxies are more clustered than the mass distribution as seems necessary for this particular scenario (Bardeen, 1986; Kaiser, 1986, Davis et. al. 1985). With this proviso, the "galaxies trace the mass" assumption gives an r.m.s. temperature fluctuation, at a point, of 1.6×10^{-5} and an r.m.s. fractional polarization of 1.0×10^{-6}. Lowering h will cause these numbers to increase (roughly like h^{-1}); varying Ω_B will not cause a significant change provided $\Omega_B \lesssim 0.2$.

Uson and Wilkinson's experiment does not provide a strong constraint on this model because the beam throw of their radio telescope (4.5') is very much smaller than the typical size of the fluctuations shown in Figure 4. An analogy can be drawn between fine-scale beam-switching experiments and an ant crawling over a

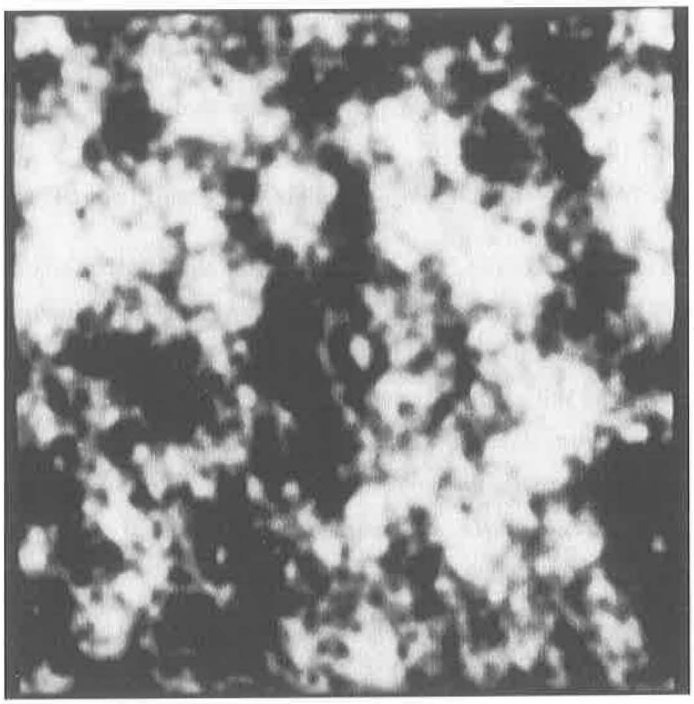

Figure 4. Simulation of the fluctuations in the radiation brightness for the scale-invariant cold dark matter model described in the text. The simulated square corresponds to an area of $10^{\circ} \times 10^{\circ}$.

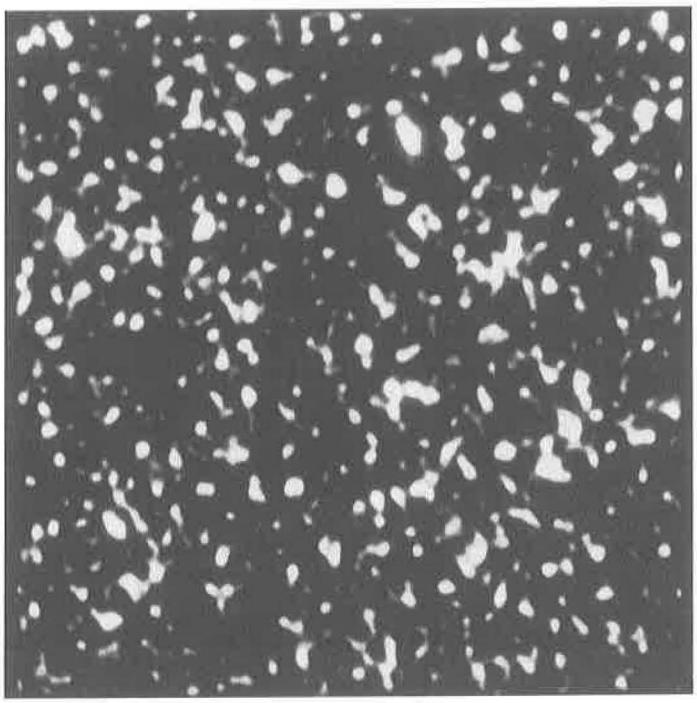

Figure 5. Map of the fractional polarization in the patch of sky shown in Figure (4).

molehill - the ant is aware of the local gradient but not its absolute height above ground level. The particular three-beam configuration used by Uson and Wilkinson is somewhat worse than this analogy suggests since it effectively measures the second derivative of the sky fluctuations. The model shown in Figure 4 predicts 2.8×10^{-6} for the Uson-Wilkinson experimental set-up.

For scale-invariant initial conditions, the quadrupole component a_2 should be considerably smaller than the r.m.s. fluctutation at a point (eq. (9), Figure 1). The current limits are $a_2 < 1.1\times10^{-4}$ (e.g. Fixsen et. al., 1983), and are well above the theoretical prediction ($a_2 = 4.9\times10^{-6}$). Subtraction of the background signal from our Galaxy is a major limiting factor in such large-angle experiments and a substantial improvement in the quadrupole limit would seem a formidable task. The large-angle experiments are capable of providing anisotropy limits on all scales larger than the effective beam-width (typically $\gtrsim5°$). For example, Fixsen. et. al. quote an upper-limit of $C_T(\vartheta)^{\frac{1}{2}} < 4\times10^{-5}$ on scales $10° < \vartheta < 180°$ after subtraction of the dipole component. Provided background emission can be adequately subtracted (perhaps by using multi-frequency observations) such limits could lead to strong constraints on scale-invariant fluctuations.

Valuable results are likely to be achieved by experiments that beam-switch on scales of $\vartheta \gtrsim 1°$, i.e. comparable to the sizes of typical clumps shown in Figure (4). As mentioned in Section (1), reionization could erase radiation anisotropies on angular scales of at most a few degrees, thus providing an additional reason to focus experiments on relatively large angular scales. The most sensitive experiment at intermediate angular scales ($\vartheta = 6°$, Melchiorri et. al., 1981) reports a detection at the level $(4.1 \pm 0.7)\times10^{-5}$. The correponding prediction for the model in Figure (4) is $\sim1\times10^{-5}$ (with an uncertainty arising from the beam width of this experiment), so it would seem unlikely that their detection is caused by the anisotropies described here, though the numbers are interestingly close. (It is quite plausible that their signal is caused by emission from dust in our Galaxy). The lack of experiments at these angular scales is partly a result of technical difficulties: a horn with a beam width of 1° would be several feet long and therefore cumbersome in a balloon borne experiment; an alternative might be to use a small dish, either in a balloon borne experiment or at a high altitude site. Another strategy might be to use a dedicated low-resolution interferometer capable of surveying a relatively large patch of sky, say 1°x1° (Lasenby, private communication). There is considerable scope for novel experiments at angular scales of one to a few degrees and it seems plausible that they could achieve the level of sensitivity required to detect anisotropies from scale-invariant initial conditions.

The polarization pattern might also provide an interesting direction for future experiments with large radio telescopes. Although the effect is considerably smaller that the total fluctuation, no beam switching is necessary to determine a temperature difference. Further, the contribution to the polarization by discrete sources is likely to be very small. The main limiting factor in such an experiment would result from instrumental polarization such as asymmetries in the antenna feeds. One way of removing these effects, to first order, might be to difference the results from well separated patches of sky.

In summary, we have attempted to show how a particular set of initial conditions in the early universe leads to a specific and therefore recognisable pattern in the microwave background radiation. An alternative way of testing initial conditions is to follow the non-linear evolution of galaxy clustering (e.g. Davis et. al., 1985). However, this approach is unlikely to lead to conclusive results because we can never be sure that the galaxy distribution is a faithful representation of the mass distribution. The microwave background radiation provides a much more direct test. A positive detection of the radiation anisotropies would revolutionise the study of galaxy formation and would have profound implications for particle physics.

Aknowledgments. This work is part of a collaborative project with J. Richard Bond. I thank Bruce Partridge for discussions about experimental configurations.

References

Bardeen, J.M., 1986, in proceedings of the Inner Space/Outer Space workshop, Fermilab, University of Chicago Press, in press.

Bardeen, J.M., Steinhardt, P.J., and Turner, M.S., 1983, Phys. Rev. D., **28**, 679.

Bond, J.R. and Efstathiou, G., 1984, Ap.J. (Letters), **285**, L45.

Bond, J.R. and Efstathiou, G., 1986, in preparation.

Davis, M., Efstathiou, G., Frenk, C.S. and White, S.D.M., 1985, Ap. J., 292, 371.

Efstathiou, G. and Bond, J.R., 1986a, Proc. Roy. Soc., in press.

Efstathiou, G. and Bond, J.R., 1986b, M.N.R.A.S., **218**, 103.

Fixsen, D.J., Cheng, E.S. and Wilkinson, D.T., 1983, Phys. Rev. Lett., **50**, 620.

Guth, A., and Pi, S.Y., 1982, Phys. Rev. D., **23**, 347.

Hawking, S., 1982, Phys. Lett., **115B**, 295.

Kaiser, N, 1983, M.N.R.A.S., **202**, 1169.

Kaiser, N., 1986, in proceedings of the Inner Space/Outer Space workshop, Fermilab, University of Chicago Press, in press.

Melchiorri, F., Melchiorri, B.O., Ceccarelli, C. and Pietranera, L., 1981, Ap. J. (Letters), **250**, L1.

Peebles, P.J.E., 1982, Ap. J. (Letters), **263**, L1.

Sachs, R.K. and Wolfe, A. M., 1967, Ap. J., **147**, 73.

Uson, J. and Wilkinson, D.T., 1984a, Ap.J. (Letters), **277**, L1.

Uson, J. and Wilkinson, D.T., 1984b, Nature, **312**, 427.

Vittorio, N. and Silk, J., 1984, Ap. J. (Letters), **285**, L39.

Wilson, M.L. and Silk, J., 1981, Ap. J., **243**, 14.